Full Paper

Shock Wave and Detonation Properties of Pressed Hydrazine Nitrate

Alexander V. Utkin[a, b] and Valentina M. Mochalova(s)*[a, b]

Abstract: In this work, the structure of the steady-state detonation waves, the critical diameter, detonation parameters and the dependence of detonation velocity on the charge diameter for pressed hydrazine nitrate (HN) charges in the density range of 1.40–1.68 g/cm^3 were investigated by VISAR interferometer. It was found that the critical diameter drops with the initial density decrease. Under steady-state detonation conditions at a maximum initial density of 1.68 g/cm^3, a high detonation velocity of 8.92 km/s is realized in HN charges. The change of the detonation velocity with variation of the initial density is not monotonic, but has a characteristic s-shape. Experiments on the determination of Hugoniot data and initiation of detonation under shock wave action for HN were carried out with samples of maximum density. The results of the conducted experiments show the low shock wave sensitivity, which is much lower than that of TNT. A noticeable reaction rate behind the front of the initiating shock wave in charges of maximum density is observed only at a pressure above 20 GPa.

Keywords: hydrazine nitrate · detonation · shock wave initiation · critical diameter · VISAR interferometer

1 Introduction

Hydrazine nitrate (HN) $N_2H_4 \cdot HNO_3$ has been studied in detail and its physicochemical properties are widely available [1–8]. The use of HN as one of the components of rocket fuels [8–12] requires the determination of their detonation parameters, sensitivity to shock wave action and critical detonation conditions. However, the available data on the detonation properties of HN are extremely limited and they are sometimes ambiguous, what is most clearly manifested in the character of the dependence of the detonation velocity D on the initial density ρ_0. According to experimental data [13], D reaches a maximum value of 5.64 km/s at $\rho_0 = 1.3$ g/cm^3, while detonation velocities exceeding 8.5 km/s at $\rho_0 = 1.6$ g/cm^3 have been obtained [8, 14]. Furthermore, there are no existing data on the shock compressibility of HN, the critical diameter value and detonation wave structures hence this research is devoted to an experimental investigation of these issues.

2 Experimental Section

Experiments on the determination of Hugoniot data and initiation of detonation under shock wave action for HN were carried out with samples of maximum density, equal to 1.68 g/cm^3, which were prepared by pressing an HN powder with an average particle size of about 500 μm. The scheme of experiments is shown in Scheme 1. Shock waves in the investigated samples (3) were created by the collision of an aluminum projectile (1), and accelerated by the explosion products to the velocity Wi, with the metal plate (2).
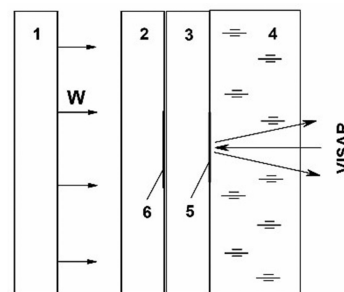
Scheme 1. Scheme of experiments for the recording of processes of detonation initiation by shock waves.

The velocity of the sample-water (4) boundary was recorded by VISAR interferometer. To determine the absolute value of the velocity, two interferometers with velocity fringe constants of 280 m/s and 1280 m/s were used simultaneously. A laser beam was reflected from an aluminum foil with a thickness of 400 μm which was glued onto the sample (5). In each experiment, the polarization gauge (6) recorded the entry time into the sample of the shock wave, which allowed us to determine the average value of the wave veloc-

[a] A. V. Utkin, V. M. Mochalova(s)
Extreme state of matter
Institute of Problems of Chemical Physics RAS
1 Semenov Ave., Chernogolovka, Russia 142432
*e-mail: roxete20000@gmail.com
[b] A. V. Utkin, V. M. Mochalova(s)
The Tomsk State University
36 Lenin Ave., Tomsk, Russia 634050

These are not the final page numbers! ↗↗

ity D_s using interferometric data. The accuracy of determination of D is higher than 1 %.

3 Results

The results of the experiments are shown in Figures 1–2 and Table 1. Table 1 shows the velocity of the aluminum projectile W_i, its thickness h_i, material and metal plate thickness h_b, sample thickness h_s. The measured values of the shock wave velocity D_s, the calculated values of the particle velocity u and the pressure P in the sample at the moment when a shock wave enters it from the metal plate are also presented. The diameters of the projectiles and samples were 70 mm and 40 mm, respectively. The designation of the velocity profiles in Figures 1–2 and the numbers of the experiments in Table 1 are the same.
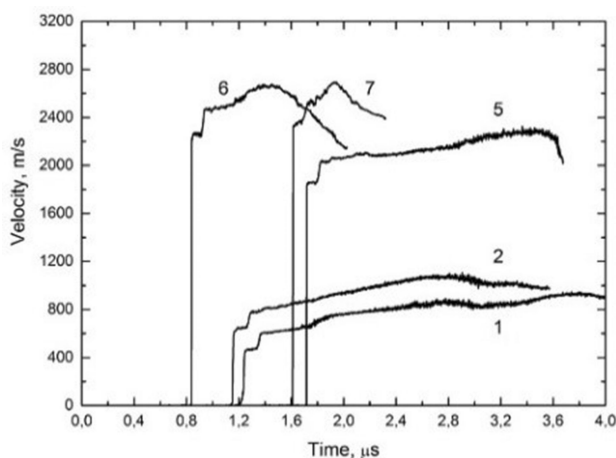
Figure 1. Particle velocity profiles on the HN/water boundary for different amplitude of initiating shock waves.
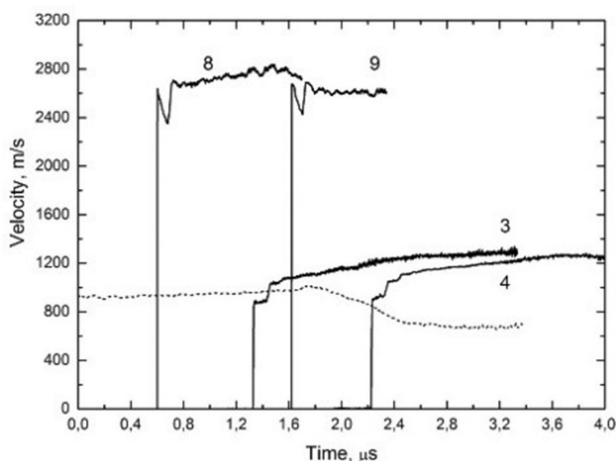
Figure 2. Particle velocity profiles on the HN/water boundary for different amplitude of initiating shock waves.

When the shock wave exits on the water boundary (Figures 1–2), the particle velocity jump is recorded, which is constant for approximately 0.1 µs (except in experiments 8 and 9), and then a second jump is observed. The formation of this velocity step at the initial moment of time is due to the reverberation of compression and rarefaction waves through the aluminum foil. Subsequent reverberations are almost not observed, and recorded velocity corresponds to the motion of the HN/water boundary. The amplitude of the initiating shock wave in experiments 1–4 is constant for approximately 1.7 µs, which is demonstrated by the dashed velocity profile in Figure 2, given for the case of the aluminum plate unloading to the water in the absence of the sample. The chemical reaction of HN behind the wave front results in a velocity increase after the shock jump, but this increase does not exceed 30 %. Moreover, in experiments 3, 4 (Figure 2), the initiation conditions are the same and only the thicknesses of the samples differ. It can be seen that an increase of the thickness of the sample from 5.80 to 9.72 mm did not result in a noticeable change in the velocity profile. This means, in particular, that under the pressure of an initiating shock wave of 5.6 GPa (experiments 3, 4), the detonation distance is more than 10 mm, whereas, for pressed TNT with density of 1.56 g/cm³, under similar conditions, it is less than 5 mm [15].

A similar character of the reaction development behind the shock wave remains the same up to a pressure of more than 15 GPa (experiment 5, Figure 1), and there is only a noticeable acceleration of the reaction rate at 20 GPa (experiments 6, 7). This results in a positive velocity gradient immediately behind the shock jump and the wave amplitude increase during its propagation through the sample. Comparing experiments 6 and 7 it follows that an increase of the thickness of the sample approximately by two times resulted in an increase of the average velocity of the shock wave by 4 %.

At a further but insignificant increase of pressure, the reaction rate increases sharply, which is manifested in a qualitative change in the velocity profiles. In experiment 8 in Figure 2, even at a sample thickness of 5 mm the velocity behind the shock jump does not increase, but rather decreases, with the formation of a character velocity peak. This means that a steady-state detonation wave with a von Neumann spike in the reaction zone is realized. The stability is evidenced by the invariance of the wave profile with an increase of the sample thickness up to 15 mm (experiment 9). It is impossible to calculate the parameters of the shock wave entering the sample in this case, based only on the measured values of D_s, but an estimate, using the Hugoniot data of HN obtained below, shows that the pressure is about 22 GPa.

As already noted, the measured values of the shock wave velocity in the sample D_s and the velocity of the projectile W_i allow us to determine the particle velocity u and the pressure P. Registration of the velocity at the boundary with the window (Figures 1–2) gives an additional possi-

↖↖ **These are not the final page numbers!**

Table 1. Parameters of setups in experiments on shock wave initiation of detonation.

N°	W_i, km/s	h_i, mm	h_b, mm	h_s, mm	D_s, km/s	u, km/s	P, GPa
1	1.13	7	Ta, 6.0	4.83	3.97	0.45	3.0
2	1.13	7	Cu, 5.5	4.75	4.21	0.57	4.0
3	1.13	7	Al, 4.0	5.80	4.36	0.77	5.6
4	1.13	7	Al, 4.0	9.72	4.38	0.77	5.6
5	2.50	10	Al, 4.0	9.50	5.55	1.64	15.1
6	3.30	5	Ti, 3.0	5.01	6.04	2.00	20.0
7	3.30	5	Ti, 3.0	9.65	6.28	1.99	21.1
8	3.30	5	Al, 4.0	5.00	8.33	–	–
9	3.30	5	Al, 4.0	14.2	8.76	–	–

bility of an independent estimation of the shock Hugoniot parameters, which increases the reliability of the results. Hugoniot parameters of HN in the coordinates of D_s-u are shown in Figure 3. The filled circles represent experimental data corresponding to a pressure below 20 GPa, at which the reaction does not result in a noticeable acceleration of the wave, and the measured average velocity D_s is almost constant when passing through the thickness of the sample. Therefore, the results of experiments 7–9, which do not satisfy this condition, are excluded from any consideration. The solid line represents a linear approximation of the experimental data: $D_s = 3.35 + 1.35u$, km/s.
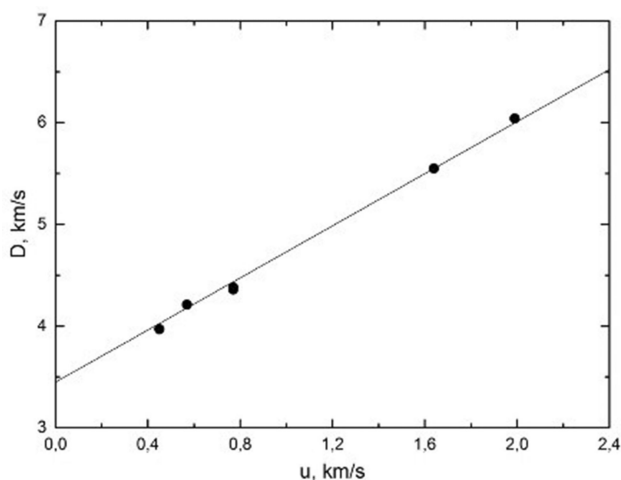
Figure 3. Hugoniot parameters of HN with a density of 1.68 g/cm^3.

The scheme of the experiments on the structure determination of the steady-state detonation waves is shown in Scheme 2. In the experiments, pressed HN charges with an initial density in the range of 1.4 g/cm^3 to 1.68 g/cm^3 were used. The charge consists of three samples of HN, the thickness of each of being equal to the radius. The plane wave generator (1) and the pressed charge of the retarded RDX (2) were used to initiate detonation in the investigated explosive. The laser beam was reflected from aluminum foil (3) with a thickness of 400 μm that was placed between the
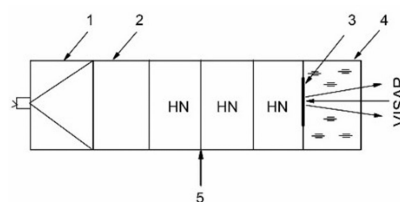

Scheme 2. Scheme of experiments for investigation of the reaction zone structure of steady-state detonation waves.

end of the charge and the water window (4). Using the ionization gauge (5), the detonation velocity was measured in each experiment.
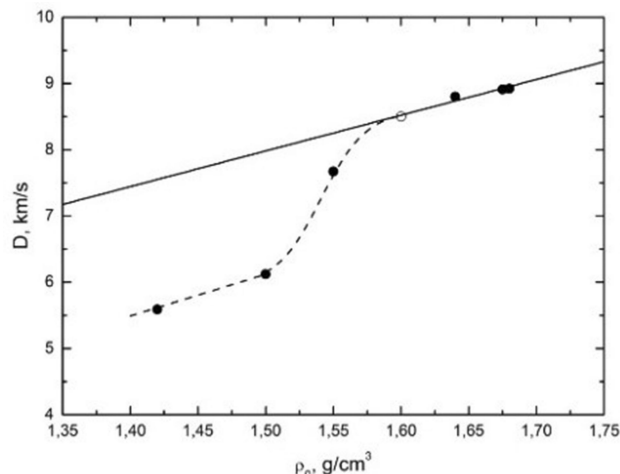
The experiments results are shown in Figures 4–8 and Table 2. Table 2 shows the initial density of the HN samples, the diameter of the charges Ø, the detonation velocity, the particle velocity u_{CJ}, and the P_{CJ} pressure at the Chapman-Jouguet (C–J) point. The parameters of the C–J point were calculated on the basis of the measured particle velocity profiles and D. At the same time, the unloading isentrope of the explosion products was approximated by the polytropic
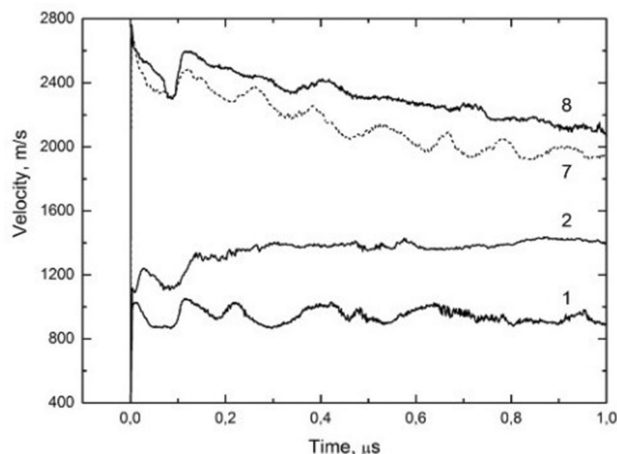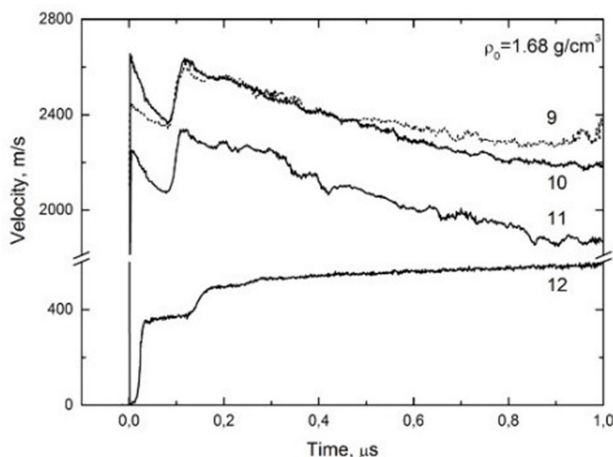

Figure 4. Particle velocity profiles on the HN/water boundary for steady-state detonation of HN charges at different densities and charge diameters.
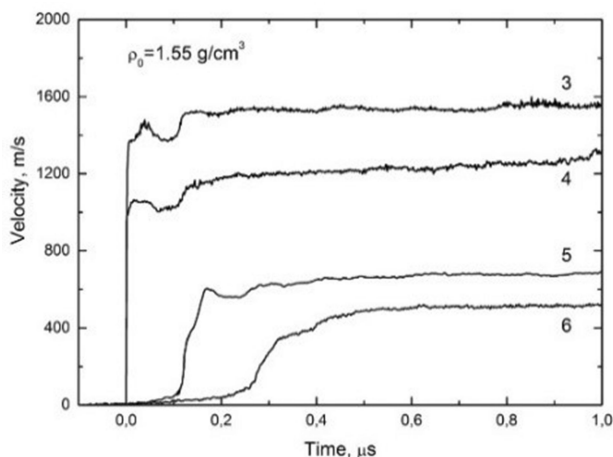
Figure 5. Particle velocity profiles on the HN/water boundary for steady-state detonation of HN charges with density of 1.55 g/cm³ for different charge diameters.

Figure 6. Particle velocity profiles on the HN/water boundary for steady-state detonation of HN charges with density of 1.68 g/cm³ for different charge diameters.

Figure 7. The dependence of detonation velocity on the initial density of HN. The empty circle relates to previously published data [8, 14].
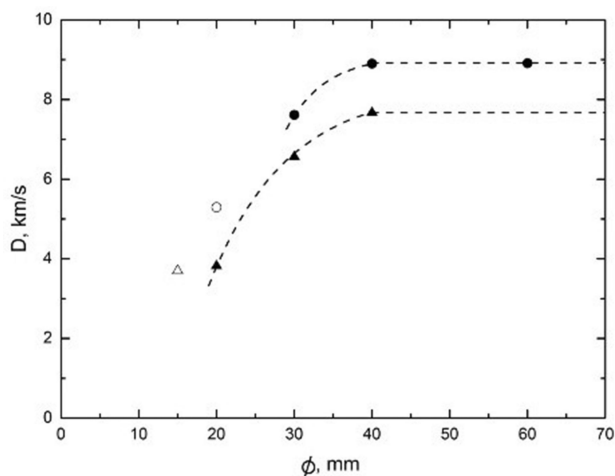
Figure 8. The dependence of detonation velocity on the charge diameter at a density of 1.68 g/cm³ (filled circles) and 1.55 g/cm³ (solid triangles).

PV^n = constant. Varying n in the range from 3 to 5 results in a change in the parameters, which is much smaller than the error shown in Table 2. The primary error is due to the accuracy of the measurement of values and the uncertainty of the C—J point position. The designation of the velocity profiles in Figures 4–6 and the numbers of the experiments in Table 2 are the same.

At an initial density of 1.64 g/cm³ and at higher initial densities, the structure of the velocity profiles has a shape that is typical of pressed explosives [16]. The velocity behind the shock jump decreases, and the von Neumann spike is formed in the reaction zone. A sharp increase in the velocity at a time of 0.1 μs, as noted above, is due to the reverberation of waves in the aluminum foil. The end of the reaction zone and the transition to the unloading wave (the

C—J point position) on the velocity profiles is not noticeable, and there are certain difficulties in estimating the character of the reaction time. To solve this problem, in this case, the approach proposed in previous research [17] is realized, which is based on a comparison of velocity profiles obtained for charges of different diameters. If the detonation parameters remain constant, the flow in the reaction zone does not depend on the diameter, whereas in the unloading wave the flow changes, what makes it possible to determine the position of the C—J point.

The velocity profiles with density of 1.68 g/cm³ for different charge diameters are shown in Figure 6. In experiments 9 and 10, the diameters differ by a factor of 1.5, while the detonation velocity is the same. The velocity profiles at

Table 2. Detonation parameters of HN.

N°	ρ_0, g/cm^3	Ø, mm	D, km/s	u_{CJ}, km/s	P_{CJ}, GPa
1	1.415	40	5.59 ± 0.05	0.63 ± 0.03	5.0 ± 0.2
2	1.50	40	6.12 ± 0.05	0.96 ± 0.03	8.8 ± 0.3
3	1.55	40	7.67 ± 0.05	1.05 ± 0.03	14.5 ± 0.3
4	1.55	30	6.56 ± 0.05	0.84 ± 0.03	8.6 ± 0.3
5	1.55	20	3.82 ± 0.05	0.5 ± 0.030	2.9 ± 0.3
6	1.55	15	3.70 ± 0.05	–	–
7	1.64	40	8.80 ± 0.05	1.45 ± 0.03	21.1 ± 0.4
8	1.675	40	8.91 ± 0.05	1.63 ± 0.03	24.4 ± 0.4
9	1.68	60	8.92 ± 0.05	1.63 ± 0.03	24.4 ± 0.4
10	1.68	40	8.92 ± 0.05	1.63 ± 0.03	24.4 ± 0.4
11	1.68	30	7.61 ± 0.05	1.47 ± 0.03	18.7 ± 0.4
12	1.68	20	5.29 ± 0.05	–	–

the border with the window also coincide, at least in the range from 0.1 µs to 0.5 µs. A noticeable discrepancy is due to the influence of the charge diameter on the velocity gradient in the unloading wave which begins at large time values. This suggests that the characteristic reaction time is approximately 0.5 µs. It is noteworthy that immediately after the shock jump, the amplitude values of the von Neumann spike in experiments 9 and 10 do not coincide, which is due to the reproducibility of the experimental results. This is confirmed by comparison of experiments 8 and 10, in which the diameters of the charges are equal, and the initial densities and detonation velocities are almost the same. The velocity profiles 8 and 10 coincide with good accuracy, except for the amplitude values of the von Neumann spike during the first 0.1 µs. It is noteworthy that in this case, the use of a relatively thick Al foil, with a thickness of 400 µm, does not result in a significant error in determination of the C–J point. This is due to the fact that the reaction time is significantly, approximately 5 times, greater than the time of the waves reverberation in the aluminum foil. Therefore, as shown in [18], where aluminum foils with a thickness from 7 to 400 µm were used, the waves reverberation in the foil does not affect the correct determination of the C–J point position.

A decrease in the initial density of HN charges not only results in the decrease of absolute values of the particle velocity, but also changes the characteristics of the dependence of velocity on time. Directly behind the shock wave, the von Neumann spike is still recorded, which is much less pronounced than in experiments with high density. Moreover, the velocity is constant or oscillates near the mean value (experiments 1–5 in Figures 4 and 5) during the entire recording time. The absence of the influence of the unloading wave, which should reduce the parameters outside the reaction zone, may be due to the increase in reaction time, because the C–J point moves to later times. However, this then means that the flow in the reaction zone, the duration of which exceeds 1 µs, does not correspond to the classical detonation model, according to which there is a decrease of particle velocity during the chemical reaction.

The measured values of the detonation velocity as a function of the initial density, with a charge diameter of 40 mm, are shown in Figure 7. A distinctive feature of the obtained results is a sharp increase of D in the density range of 1.5–1.6 g/cm^3. Moreover, this effect is not a consequence of the influence of the charge diameter on the detonation velocity. This is evidenced by the data shown in Figure 8, where the filled circles represent the detonation velocity dependence on the charge diameter for the HN initial density of 1.68 g/cm^3. It can be seen that the detonation velocity is constant at diameters of 40 mm and greater. This gives reason to believe that the measured value D = 8.92 km/s is the maximum and corresponds to ideal detonation. Reduction of the charge diameter up to 30 mm results in a marked decrease of the detonation velocity (experiment 11), and at 20 mm (experiment 12) the detonation attenuates; the measured velocity is shown in Figure 8 by empty circle. The velocity profiles at the HN/water boundary also change accordingly. In experiment 11 (Figure 6), the particle velocity decreases, remaining qualitatively similar to profile 10, whereas in experiment 12 its time dependence varies qualitatively: after a shock jump a monotonic increase of velocity is observed instead of a von Neumann spike. Thus, the critical diameter of HN with a density of 1.68 g/cm^3 is greater than 20 mm, but less than 30 mm.

An analogous detonation velocity dependence on the charge diameter is also observed at a density of 1.55 g/cm^3 (triangle points in Figure 8). In this case, detonation attenuates at a diameter of 15 mm (empty triangle), whereas at a diameter of 20 mm or more a steady-state detonation regime is established. With a decrease of the charge diameter from 40 to 20 mm (experiments 3, 4, 5 in Figure 5) the velocity profiles are qualitatively similar and only absolute values of the particle velocity decrease. At the same time, with a charge diameter of 15 mm (experiment 6 in Figure 5), the time dependence, as with the density of 1.68 g/cm^3 at Ø = 20 mm, changes qualitatively, the von Neumann spike disappears and the velocity increases monotonically after the shock jump, i.e., the critical diameter at a density of 1.55 g/cm^3 is greater than 15 mm, but less than 20 mm.

Two obtained results – the drop in the critical diameter with the initial density decrease and the independence of D on the charge diameter at Ø 40 mm for a maximum density of 1.68 g/cm³ – suggest that the D (ρ_0) dependence (shown in Figure 7) corresponds to an infinite diameter. Indeed, with density decrease, the diameter of the charge Ø = 40 mm is increasingly moved from the critical value, and, consequently, the influence of diameter on the detonation velocity is increasingly diminished.

The charge diameter decrease not only results in a change in the character of the flow behind the shock wave, but it also results in a change in the front structure, what is especially noticeable at the density of 1.55 g/cm³ for diameters of 20 mm and 15 mm (experiments 5, 6 in Figure 5). Unlike the velocity profiles obtained for large diameters, in this case a two-wave configuration is formed. Further, the first wave is not shock-related, the particle velocity smoothly increases from zero to the maximum value, which is reached before the front of the second wave. Such a structure of the compression pulse is typical for porous media and it can be seen more clearly at the wave amplitude decrease.

4 Discussion and Conclusions

The results of the conducted experiments show that the detonation properties of HN have a number of features. Firstly, the low shock wave sensitivity is noteworthy, which is much lower than that of TNT. A noticeable reaction rate behind the front of the initiating shock wave in charges of maximum density is observed only at a pressure above 20 GPa. With a further pressure increase by only a few GPa, the exit distance to the steady state regime is reduced several times, i.e. reliable initiation of detonation is realized only when the initiating pressure is slight, 10–15 % below the parameters at the C—J point. A similar characteristic of detonation development during shock wave action is usually observed in liquid high explosives [19]. It is noteworthy, however, that even at low pressures (3–5 GPa) the velocity behind the shock wave front increases (Figures 2–3), which indicates the decomposition of HN with energy release. The low rate of the chemical reaction and the finite duration of the initiating compression pulse do not permit observation of the possible exit to the steady-state detonation regime in this case; nevertheless, it can be assumed that the initiation threshold of the reaction in HN does not exceed 3 GPa.

Under steady-state detonation conditions at an initial density of 1.68 g/cm³, a high detonation velocity of 8.92 km/s is realized in HN charges. The pressure at the C—J point does not exceed 25 GPa, which corresponds to the value of the polytropic exponent close to 4.5. The change of the detonation velocity with variation of the initial density is not monotonic, but has a characteristic s-shape: D increases sharply with increasing ρ_0 in the density range of 1.5–1.6 g/cm³ (Figure 7). Such a dependence of D (ρ_0) does not allow us to relate HN to the second group of high explosives, as has been suggested in previous research [20], since the data given in Figure 7 were obtained with a fixed charge diameter and should lie either on the linear dependence D(ρ_0) (ideal detonation), or on the dependence with the maximum, which was observed in previous research [14] for HN charges with a diameter of 41.4 mm. Such a significant discrepancy between the experimental data is probably due either to the structure of the investigated samples (for example, the particle size) or to the conditions for the undertaking of experiments. It is also noteworthy that the dependence D = 5.388·ρ_0–0.100 km/s, where ρ_0 is in g/cm³, that has been proposed in previous research [14] for the ideal detonation of HN and is shown by the solid line in Figure 7, agrees well with the results of the present work at $\rho_0 > 1.6$ g/cm³.

Despite the complex character of the obtained D(ρ_0) dependence, it is not a unique feature of HN. A similar characteristic of the detonation velocity change with the initial density variation was observed in previous research [21] for nitroguanidine. In the interval of 1.30–1.62 g/cm³, the experimental data for nitroguanidine lie on the D(ρ_0) dependence corresponding to the ideal detonation, but at $p_0 < 1.2$ g/cm³ the detonation velocity decreases sharply, and in previous research [21] this has been related to the realization of the low-velocity detonation regime. It is probable that a similar regime is realized in HN at $\rho_0 < 1.5$ g/cm³. Low-velocity detonation is observed for many types of condensed energy materials, including liquid and solid high explosives [21]. Steady-state propagation of detonation with low velocity is observed for certain values of the particle size of high explosive and the charge diameter. In the present work, we used HN with a sufficiently large crystalline particle size (~ 0.5 mm), which probably explains the difference between the obtained dependence D(ρ_0) and some results of previous research [14].

With respect to the example of nitroguanidine, it has been demonstrated [22] that in different intervals of the initial density, the properties of high explosives can correspond to different groups of explosives. This conclusion also applies to HN, whose critical diameter increases with initial density increase, at least for $\rho_0 \geq 1.55$ g/cm³, which is typical for high explosives of the 2nd group.

References

[1] L. F. Audrieth, B. A. Ogg, *The Chemistry of Hydrazine*, John Wiley & Sons, New York, **1951**, p. 238.

[2] L. I. Khmelnitskiy, *Handbook of High Explosives. Part 2:* (Eds: Novikov S. S.), Moscow, **1962**, p. 829.

[3] S. F. Sarner, *Propellant Chemistry*, Reinhold publishing corp., New York, **1966**, p. 297.

[4] J. Liu, *Liquid Explosives*, Springer, **2015**.

[5] T. M. Klapötke, C. M. Rienäcker, H. Zewen, *Calculated and Experimentally Obtained Heats of Combustion of Hydrazinium Nitrate, Monomethylhydrazinium Nitrate, and N,N-Dimethylhydrazinium, Nitrate Anorg. Allg. Chem.* **2002**, *628*, 2372–2374.

[6] R. J. Robinson, W. C. McCrone, *Anal. Chem.* **1958**, *30*, 1014–1015.

[7] A. A. Shklovskiy, V. I. Semishin, V. I. Simutin, *Thermal decomposition and combustion of hydrazine nitrate, J. Appl. Chem.* **1960**, *33*, 1411–1413.

[8] Y. Miron, H. E. Perlee. *The Hard Start Phenomena in Hypergolic. Engines Volume 3: Physical and Combustion Characteristics of Engine Residuals*, NASA CR-140361, USA, **1974**.

[9] L. F. A. Urbana, D. W. Ryker, *Fuel*, United States Patent Office 2943927, USA, **1960**.

[10] Vernon E. Haury, David R. V. Golding, *Solid propellant containing fuel-oxidizer component prepared from fused oxidizers*, United States Patent Office 3837938, USA, **1974**.

[11] T. Paine, W. W. Thompson, *Inhibited solid propellant composition containing beryllium*, United States Patent Office 4111729, USA, **1978**.

[12] R. S. Bruenner, A. E. Oberth, G. M. Clark, A. Katzakian, *Liquid nitrate oxidizer compositions,* United States Patent Office 5734124, USA, **1998**.

[13] L. Medard, *Hydrazine (Explosive Properties of Hydrazine Nitrate), Meml. Poudres* **1952**, *34*, 147–157.

[14] D. Price, T. P. Liddiard, Jr., R. D. Drosd, *The Detonation Behavior of Hydrazine Mononitrate*, U.S. Naval Ordnance Lab., Rept. NOLTR-66-31, USA, **1966**.

[15] L. P. Orlenko. *Explosion Physics* Fizmatlit, Moscow, **2002**, p. 822.

[16] A. V. Utkin, S. A. Kolesnikov, S. V. Pershin, *Effect of the Initial Density on the Structure of Detonation Waves in Heterogeneous Explosives, Combust. Explos. Shock Waves (Engl. Transl.)* **2002**, *38*, 590–597.

[17] V. M. Mochalova, A. V. Utkin, S. M. Lapin, *Effect of small additions of diethylenetriamine on the width of the reaction zone in detonation waves in nitromethane, Combust. Explos. Shock Waves (Engl. Transl.)* **2016**, *52*, 329–334.

[18] S. I. Torunov, A. V. Utkin, V. M. Mochalova, V. A. Garanin, *Combust. Explos. Shock Waves (Engl. Transl.)* **2010**, *46*, 599–603.

[19] A. N. Dremin, S. D. Savrov, V. S. Trofimov, K. K. Shvedov, *Detonation waves in condensed matter*, Science, Moscow, **1970** p. 154.

[20] D. Price, *Contrasting patterns in the behavior of high explosives, Combust., [Int. Symp.]* **1967**, *11*, 693–702.

[21] D. Price, A. R. Clairmont Jr., *Explosive behavior of nitroguanidine, Combust., [Int. Symp.]* **1969**, *12*, 761–770.

[22] A. F. Belyaev, V. K. Bobolev, A. I. Korotkov, A. A. Sulimov, S. V. Chuiko, *The transition of combustion to an explosion for condensed systems*, Science, Moscow, **1973**.

FULL PAPER
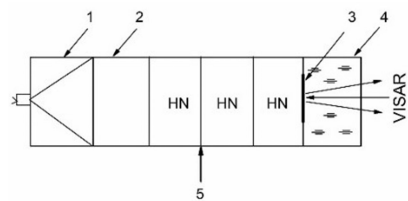
A. V. Utkin, V. M. Mochalova*

1 – 8

Shock Wave and Detonation Properties of Pressed Hydrazine Nitrate